ISSN 0036-0244, Russian Journal of Physical Chemistry A, 2011, Vol. 85, No. 5, pp. 751–759. © Pleiades Publishing, Ltd., 2011.
Original Russian Text © M.F. Butman, V.B. Motalov, D.N. Sergeev, L.S. Kudin, K.W. Krämer, 2011, published in Zhurnal Fizicheskoi Khimii, 2011, Vol. 85, No. 5, pp. 838–846.

CHEMICAL THERMODYNAMICS AND THERMOCHEMISTRY

Composition of Saturated Vapor over Ytterbium Bromides

M. F. Butman[a], V. B. Motalov[a], D. N. Sergeev[a], L. S. Kudin[a], and K. W. Krämer[b]

[a] *Ivanovo State University of Chemistry and Technology, pr. Engelsa 7, Ivanovo, 153000 Russia*
e-mail: butman@isuct.ru

[b] *Department of Chemistry, University of Bern, Bern, Switzerland*
e-mail: karl.kraemer@iac.unibe.ch

Received April 23, 2010

Abstract—The vaporization process of ytterbium di- and tribromide was studied using high-temperature mass spectrometry over the temperature range of 850 to 1300 K. It was ascertained that, at the early vaporization stages, the vapor contained molecules $YbBr_3$, $YbBr_2$, YbBr, Br_2, Yb_2Br_2, Yb_2Br_3, Yb_2Br_4, Yb_2Br_5, Yb_2Br_6, and atoms Yb and Br. The partial pressures of all components of saturated vapor were calculated. It was found that vapor composition reflected the course of the reactions of decomposition of tribromide and disproportionation of dibromide in the condensed phase. It was concluded that vaporization of di- and tribromide was incongruent at the initial stages; vaporization of both agents acquired a congruent character with the Yb : Br = 1.0 : $1.9_{\pm 0.2}$ ratio with time.

Keywords: high-temperature mass spectrometry, ytterbium bromide, saturated vapor, vaporization, partial pressure.

DOI: 10.1134/S0036024411050062

INTRODUCTION

Lanthanide atoms are known to most likely exist in halogen compounds in stable trivalent state. The thermodynamics of vaporization of LnX_3 has recently been studied fairly completely [1–4]. Europium, ytterbium, and samarium are exceptions for which reliable thermodynamic characteristics of the vaporization process have virtually not been published. This primarily accounts for the incongruent character of evaporation [5, 6] and the valence transformation Ln(III) → Ln(II) in these compounds at high temperatures, which is in accord with the general tendency toward decreasing stability of the trivalent state in the lanthanide series [7, 8]: La, Lu, Gd, Ce, Tb, Pr, Er, Nd, Ho, Pm, Dy, Tm, Sm, Yb, and Eu. Their thermal decomposition occurs due to the decreased stability of the state of Ln(III) in trihalogenide compounds [1, 9]:

$$2LnX_3(s) \rightarrow 2LnX_2(cr) + X_2(g). \quad (1)$$

On the other hand, it was noted in [7, 10] that lanthanide dihalogenides disproportionate at high temperature via the reaction

$$3LnX_2(s) \rightarrow Ln(cr) + 2LnX_3(cr). \quad (2)$$

Unfortunately, no detailed information on the conditions of reaction (2) has been published, with the exception of data for $LnCl_2$ compounds, which disproportionate under vacuum at $T \geq 1273$ K [11, 12]. The type of reaction (2) was determined mainly by analyzing the composition of the condensed phase, whereas the composition of the gas phase during this reaction has not been investigated.

It should be noted that reactions (1) and (2) are mutually concurrent in a certain sense, since the lanthanide trihalogenide released in reaction (2) at such high temperatures must decompose via reaction (1), particularly in the presence of a metal. Thus far, no attention has been given to this in the literature, although this concurrence can result in subtle chemical effects associated with the high-temperature valence transformation of a lanthanide. In turn, this circumstance considerably complicates the investigation of vaporization regularities of individual compounds LnX_2 and LnX_3 with the valence-instable state of lanthanide. Since the composition of saturated vapor is complex and susceptible to serious changes, this type of study can be carried out only using the differential tensimetry methods, high-temperature mass spectrometry in particular [13].

In this work, the mass spectrometric investigation of regularities in vaporization of ytterbium tri- and dibromide was performed in order to determine the qualitative and quantitative composition of saturated vapor.

EXPERIMENTAL

The experiment was conducted on an MI 1201 serial magnetic mass spectrometer (∠90°, curvature radius of 200 mm) reequipped for high-temperature effusion measurements from a Knudsen cell (materials: graphite, molybdenum). The molecular and ion beams were located coaxially. The instrument was described in more detail in [14]. Mass spectra were

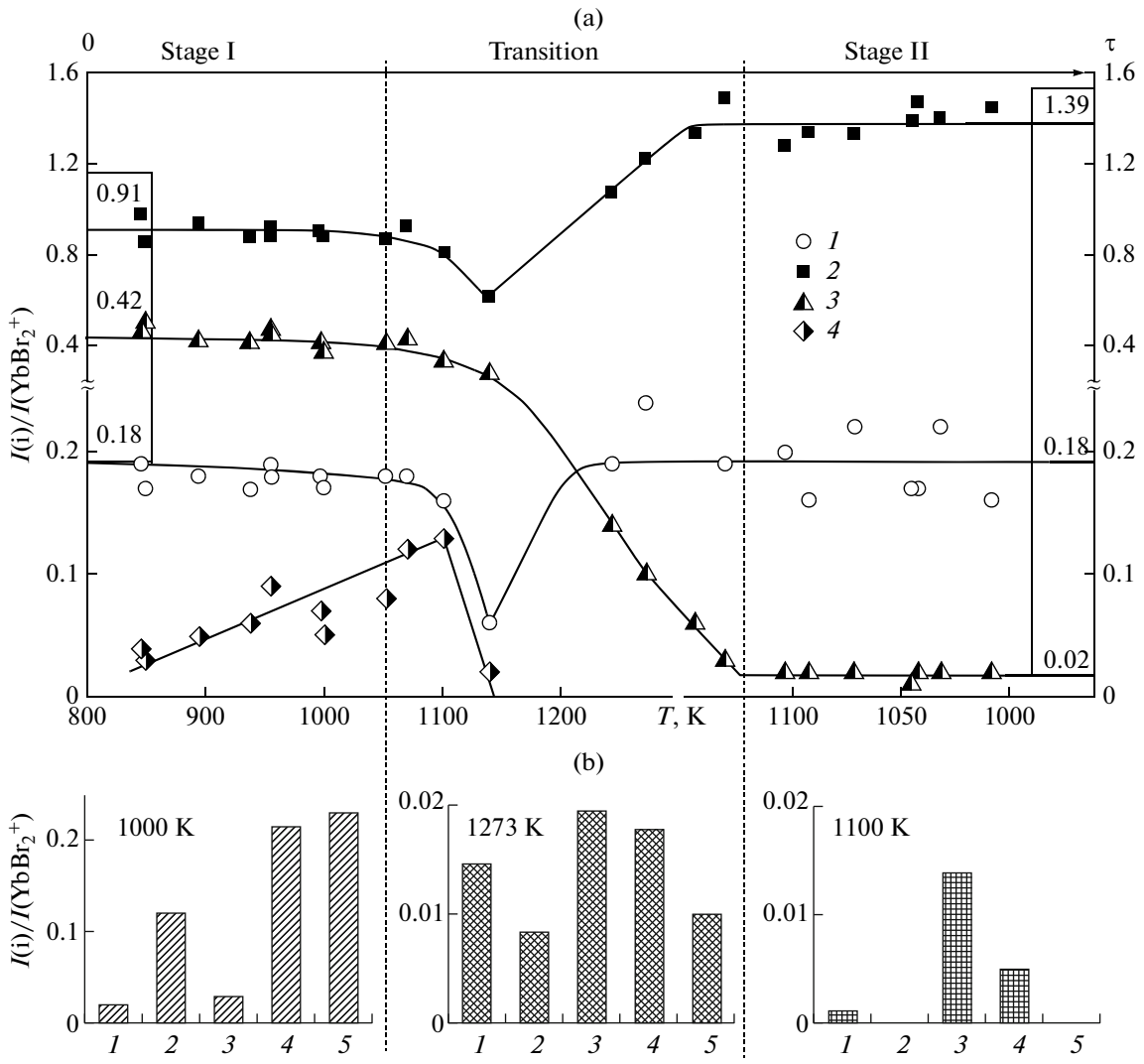

Fig. 1. Temperature dependences of the mass spectra and their change over time upon the vaporization of $YbBr_3$; (a) ion i: (*1*) Yb^+; (*2*) $YbBr^+$; (*3*) $YbBr_3^+$; (*4*) Br_2^+; (b) ion i: (*1*) Yb_2Br^+; (*2*) $Yb_2Br_2^+$; (*3*) $Yb_2Br_3^+$; (*4*) $Yb_2Br_4^+$; (*5*) $Yb_2Br_5^+$; τ is the duration of the experiment.

recorded at an energy of ionizing electrons $E_{\bar{e}} = 30$ eV, and an emission current from the cathode of I_e 1 mA. A secondary electron multiplier combined with a Keithley digital picoampermeter allowed us to attain a sensitivity of the registration system of 10^{-17} A in the direct current measurement mode. The temperature of the effusion cell was measured using a standard tungsten–rhenium thermocouple calibrated for the melting points of pure CsI and Ag. The sensitivity constant of the instrument was calibrated according to the saturated vapor pressure over metallic silver. A software module designed in our laboratory allowed automatic registering of the ion current, cell temperature, and energy of the ionizing electrons in the course of measuring.

The $YbBr_3$ sample was synthesized from Yb_2O_3 (Fluka, 99.9%) using the NH_4Br procedure [15, 16], which includes the following stages: dissolution of ytterbium oxide in concentrated (47%) HBr solution; introduction of ammonium bromide in Yb : NH_4Br ratio of 1 : 3.5, followed by vaporization of the solution; grinding of the residue and its heating to 150°C in argon flow and to 450°C under vacuum. The brutto reactions of synthesis are described by equations:

$$Yb_2O_3 + 6HBr + 6NH_4Br \rightarrow 2(NH_4)_3YbBr_6 + 3H_2O, \quad (3)$$

$$(NH_4)_3YbBr_6 \rightarrow YbBr_3 + 3NH_4Br. \quad (4)$$

For further purification, the dry $YbBr_3$ powder was sublimed in an airtight quartz reactor at 950°C under vacuum.

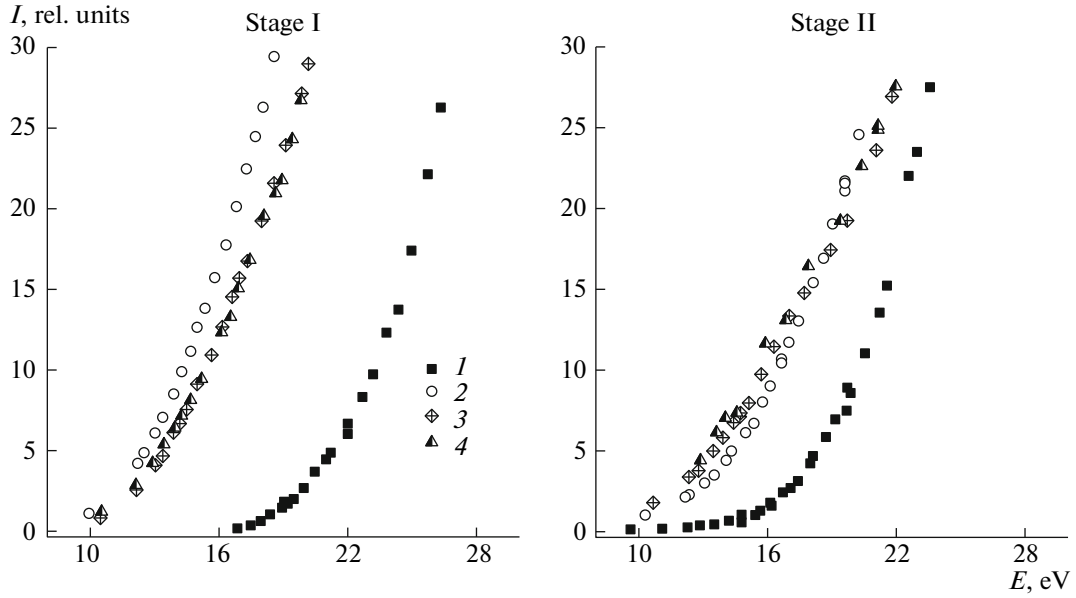

Fig. 2. Ionization efficiency curves at I and II stages of vaporization of $YbBr_3$ for ions (*1*) Yb^+; (*2*) $YbBr^+$; (*3*) $YbBr_2^+$; (*4*) $YbBr_3^+$.

The $YbBr_2$ sample was obtained by reducing $YbBr_3$ with metallic Yb (Metall Rare Earth Ltd., 99.99%) in a tantalum container sealed by arc welding in a helium atmosphere and enclosed in a quartz ampoule. The metal was used in excess $YbBr_3$: Yb ratio of 2 : 1.05. The temperature was raised to 980°C and kept there for 24 h, then lowered to 800°C and kept for 24 h followed by slow cooling to room temperature over 72 h. The resultant pale yellowish-white powder was identified via X-ray diffraction as phase pure $YbBr_2$.

RESULTS AND DISCUSSION

Mass Spectra of $YbBr_3$ Vaporization Products

The following ions were registered in the mass spectrum upon the vaporization of $YbBr_3$ over the temperature range of 850 to 1300 K: Yb^+, $YbBr^+$, $YbBr_2^+$, $YbBr_3^+$, Br_2^+, Br^+,[1] Yb_2Br^+, $Yb_2Br_2^+$, $Yb_2Br_3^+$, $Yb_2Br_4^+$, and $Yb_2Br_5^+$.

In the course of measurements, two main stages were observed; these are denoted by Roman numerals I and II in Fig. 1. Note that these and all subsequent data were obtained using a graphite cell, stage I being more prolonged than when a molybdenum cell is used, which ensures greater reliability in measuring the ratios between the ion currents in a mass spectrum.

As can be seen in Fig. 1, the mass spectra of vapor differ considerably at different stages, this distinction comprising not only the qualitative change in the ratios of ion currents but the complete vanishing of Br_2^+ and Br^+ ions from the mass spectrum at stage II as well. We note that at both stages, the mass spectra differ from those of lanthanide tribromides [17–21]. The phenomena that stand out in particular are a very high fraction of $YbBr^+$ ion and a wide variety of ions containing two ytterbium atoms. The presence of Br^+ and Br_2^+ ions at stage I indicates the release of atomic and molecular bromine[2] due to the thermal decomposition of the sample via reaction (1).

Analysis of Ionization Efficiency Curves

In order to determine the molecular precursors of ions at each vaporization stage, we recorded the ionization efficiency curves (IECs) (Fig. 2), which are the dependences of mass spectra on energy of ionizing electrons. The energy scale in Fig. 2 was calibrated with respect to the $YbBr_3^+$ ion, since it forms only as a result of the ionization of $YbBr_3$ molecules (by analogy with other lanthanide tribromides [17–21]) and corresponds to a so-called "pure line" in the mass spectrum. The ion appearance energy $AE(YbBr_3^+, YbBr_3) = 9.5 \pm 0.5$ eV, which is the same as the ionization energy I_0 of

[1] The measurements of ion current of Br^+ were complicated by considerable background noise from the instrument at m/e = 79, 81 and were performed only at several individual temperature values (not shown in Fig. 1). The atomic bromine pressure was, however, taken into account in calculating the relative content of Br/Yb atomic feractions in the vapor (see below).

[2] According to the assumption in [22] on possibility of ignoring the dissociative ionization of Br_2, the ratio between ion currents of Br^+ and Br_2^+ corresponds to the equilibrium constant of reaction $Br_2 = 2Br$.

Fragmentation coefficients of YbBr, $YbBr_2$, and $YbBr_3$ molecules

Coefficient	Value
$f_{01} = I(Yb^+,YbBr)/I(YbBr^+,YbBr)$	0.05 ± 0.02
$f_{02} = I(Yb^+,YbBr_2)/I(YbBr_2^+,YbBr_2)$	0.19 ± 0.03
$f_{03} = I(Yb^+,YbBr_3)/I(YbBr_3^+,YbBr_3)$	0.11 ± 0.03
$f_{12} = I(YbBr^+,YbBr_2)/I(YbBr_2^+,YbBr_2)$	0.90 ± 0.11
$f_{13} = I(YbBr^+,YbBr_3)/I(YbBr_3^+,YbBr_3)$	0.35 ± 0.05
$f_{23} = I(YbBr_2^+,YbBr_3)/I(YbBr_3^+,YbBr_3)$	1.24 ± 0.14

Note: $I(Yb^+, YbBr)$ is the intensity of the current of Yb^+ ions formed from YbBr molecule. The same is true for the other cases.

the $YbBr_3$ molecule, was determined by the extrapolated difference method [23] using $I_0(Br_2) = 10.53 \pm 0.01$ eV [12] as a standard. It should be noted that the *AE* values for the other ions were not determined precisely in this work, such determination being complicated under the superposing of spectra of individual molecules due to the distortion of IEC shapes. In interpreting the mass spectra, we therefore relied on our analysis of shapes and relative shifts of the IECs obtained in one experiment.

As can be seen in Fig. 2, the curve of $YbBr^+$ ion is shifted leftward at stage I and yields an *AE* value of approximately 9 eV. Note that it is the lowest value, compared to the other ions. Moreover, it is considerably lower than the values of ~15–16 and ~10–11 eV, predicted for $AE(YbBr^+, YbBr_3)$ and $AE(YbBr^+, YbBr_2)$. This demonstrates that at stage I, not only $YbBr_3$ and $YbBr_2$ but also YbBr molecules contribute to the ion current of $YbBr^+$.

In moving to stage II, the IEC of $YbBr^+$ shifts rightward and curves in more to mask its break, while the lower region of the curve can still be extrapolated into the low energy range (<9 eV). Such behavior corresponds to a relatively lower contribution to the total current of $YbBr^+$ from ytterbium monobromide at stage II. The $AE(Yb^+)$ value on the order of 15–16 eV (Fig. 2, stage I), along with the IEC shape for Yb^+ ion, demonstrates that it prefers to form at stage I from $YbBr_3$ and $YbBr_2$ molecules. At stage II, the break of the IEC of Yb^+ becomes more pronounced, and a long region extending to the low energy range emerges in the curve, attesting to the emergence of a contribution to current of Yb^+ from Yb atoms. In the case of the $YbBr_2^+$ ion, the changes in IEC at stages I and II (Fig. 2) are pronounced to a lesser extent and are manifested as a small shift of the curve (~0.5 eV) leftward, indicating a relative increase in the contribution to this ion from dibromide molecules at stage II.

The observations described above and our interpretation of them suggest that the vapor composition at which up to four ytterbium-containing gas components ($YbBr_3$, $YbBr_2$, YbBr, and Yb) can simultaneously coexist is complex. The next stage of processing the primary data therefore involved separating the contributions to ion currents from different molecular precursors.

Attribution of Ion Currents to Molecular Precursors

Let us introduce the concept of fragmentation coefficient

$$f_{ij} = I_{ij}/I_{jj}, \quad (5)$$

which determines the ratio between fragmentary $YbBr_i^+$ and molecular $YbBr_j^+$ ion currents formed from the $YbBr_j$ molecule ($i < j$). Let us express ion currents I_{03}, I_{13}, I_{23} of fragmentary ions Yb^+, $YbBr^+$, and $YbBr_2^+$, the products of ionization of $YbBr_3$ molecule, in terms of ion current I_{33} of the pure line of $YbBr_3^+$ and the corresponding fragmentation coefficient:

$$I_{i3} = f_{i3}I_{33}, \quad (i = 0, 1, 2). \quad (6)$$

Likewise, for $YbBr_2$ and YbBr molecules we obtain the expressions

$$I_{i2} = f_{i2}I_{22}, \quad (i = 0, 1); \quad (7)$$

$$I_{i1} = f_{i1}I_{11}, \quad (i = 0); \quad (8)$$

respectively. The task of attribution of ion currents to molecular precursors is thus reduced to determining the coefficients $f_{03}, f_{13}, f_{23}, f_{02}, f_{12}$, and f_{01}. With this in mind, we considered the balance equations of ion currents measured upon vaporization of $YbBr_3$ at stage I, where the content of Yb atoms in vapor could be ignored (see above):

$$I_{01} = I_0 - f_{03}I_3 - f_{02}(I_2 - f_{23}I_3), \quad (9)$$

$$I_{11} = I_1 - f_{13}I_3 - f_{12}(I_2 - f_{23}I_3), \quad (10)$$

where I_i is the measured ion current.

Substituting (9) and (10) into (8), we express

$$f_{01} = \frac{I_0 - f_{03}I_3 - f_{02}(I_2 - f_{23}I_3)}{I_1 - f_{13}I_3 - f_{12}(I_2 - f_{23}I_3)}. \quad (11)$$

Since f_{01} is independent of gas phase composition and temperature (as we assumed), expression (11) is valid for each of the experimental points at stage I. It can therefore be written for two points as

$$\frac{I_0' - f_{03}I_3' - f_{02}(I_2' - f_{23}I_3')}{I_1' - f_{13}I_3' - f_{12}(I_2' - f_{23}I_3')} = \frac{I_0'' - f_{03}I_3'' - f_{02}(I_2'' - f_{23}I_3'')}{I_1'' - f_{13}I_3'' - f_{12}(I_2'' - f_{23}I_3'')}, \quad (12)$$

where I_i' and I_i'' are the ion currents for the first and second random points. Using the experimental data

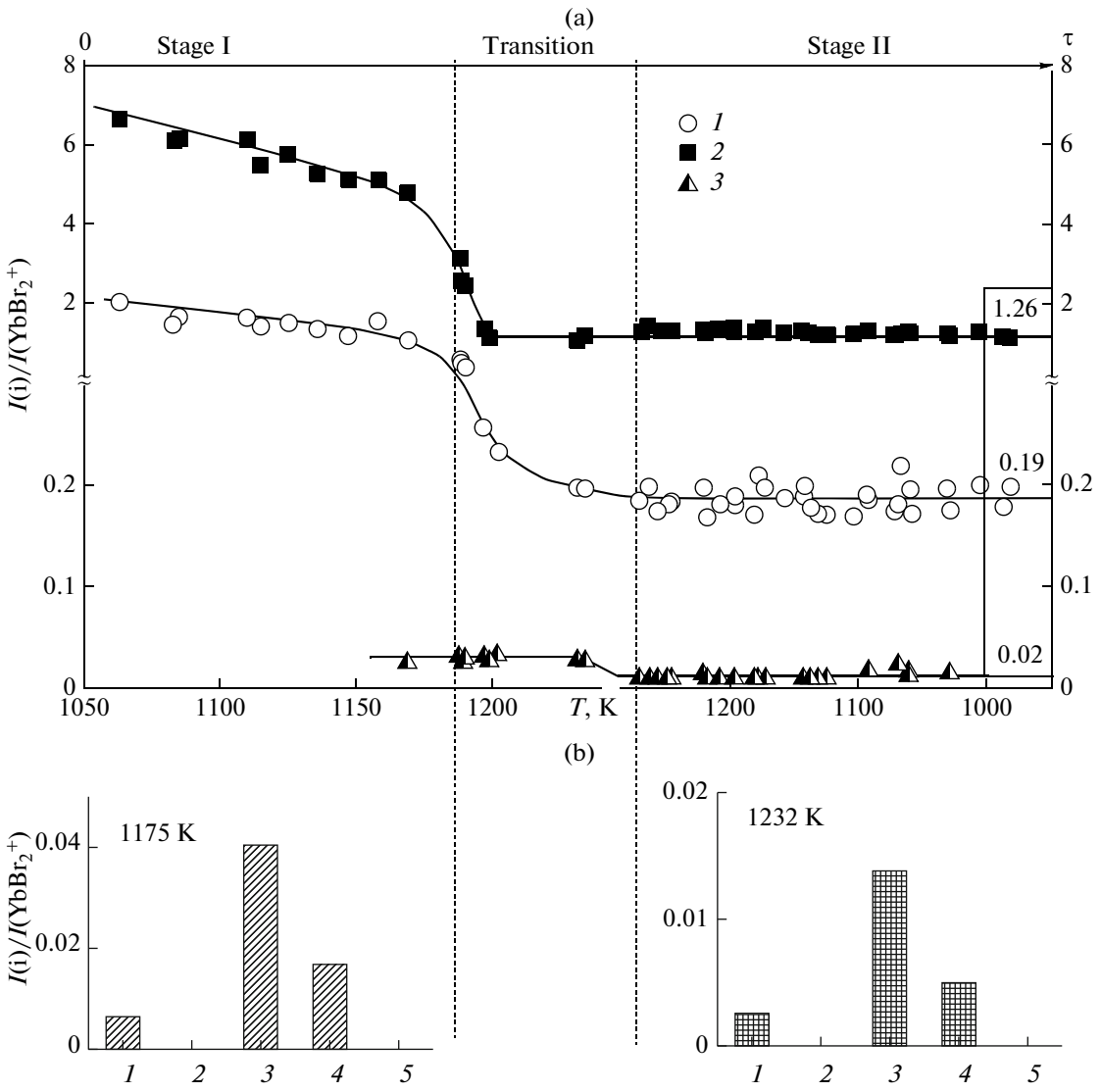

Fig. 3. Temperature dependences of the mass spectra and their change over time upon the vaporization of $YbBr_2$; (a) ion i: (*1*) Yb^+; (*2*) $YbBr^+$; (*3*) $YbBr_3^+$; (b) ion i: (*1*) Yb_2Br^+; (*2*) $Yb_2Br_2^+$; (*3*) $Yb_2Br_3^+$; (*4*) $Yb_2Br_4^+$; (*5*) $Yb_2Br_5^+$.

on ion currents measured at different temperatures, a system of type (12) nonlinear equations was devised, the Levenberg–Marquardt gradient method [24] with the criterion of allowable convergence of 0.01 being used for its resolution. The resultant fragmentation coefficients are listed in table.

Mass Spectra of the Products of Vaporization of $YbBr_2$

Yb^+, $YbBr^+$, $YbBr_2^+$, $YbBr_3^+$, Yb_2Br^+, $Yb_2Br_3^+$, and $Yb_2Br_4^+$ ions were recorded in the mass spectra in heating $YbBr_2$ over the temperature range of 1050 to 1300 K. Just as in the experiment with $YbBr_3$, the vaporization of ytterbium dibromide occurred in two stages (Fig. 3). At stage I, the relative content of $YbBr_2^+$ ions in the mass spectrum was considerably lower than that of Yb^+ and $YbBr^+$ ions. An abrupt increase in the relative signal of $YbBr_2^+$ was observed at stage II. The presence of $YbBr_3^+$ ion attests to the occurrence of $YbBr_3$ molecules in the vapor; these can be formed in reaction (2). Note that the mass spectrum at stage II appeared to be similar to the mass spectrum of vaporization of $YbBr_3$ (Fig. 1, stage II). Since the fragmentation coefficients of the molecules potentially present in the vapor were obtained earlier (see above), a deeper analysis of the mass spectra by means of the IECs would in this case have been redundant and was not performed.

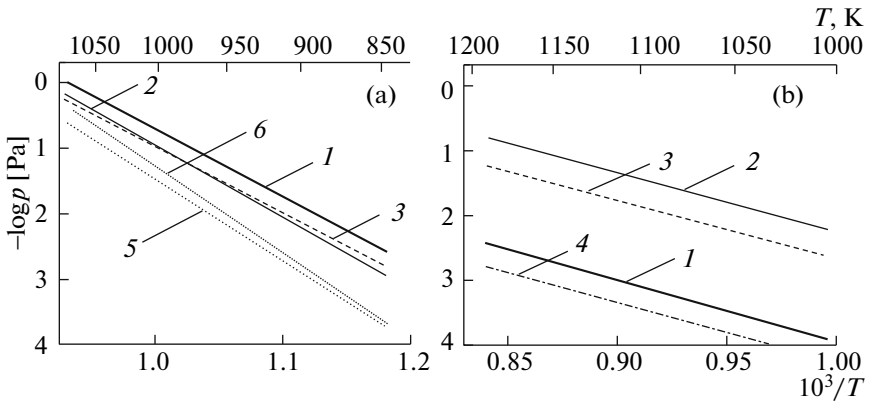

Fig. 4. Temperature dependences of partial pressures of vapor components upon the vaporization of $YbBr_3$: (*1*) $YbBr_3$; (*2*) $YbBr_2$; (*3*) YbBr; (*4*) Yb; (*5*) Br_2; (*6*) Br; stages (a) I and (b) II, respectively.

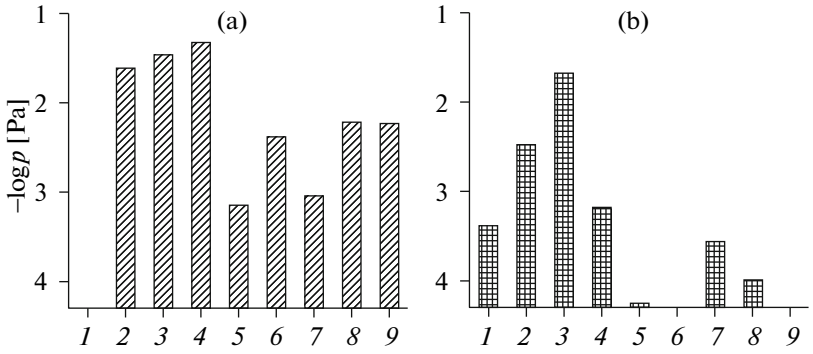

Fig. 5. Total vapor composition upon the vaporization of $YbBr_3$: (*1*) Yb; (*2*) YbBr; (*3*) $YbBr_2$; (*4*) $YbBr_3$; (*5*) Yb_2Br_2; (*6*) Yb_2Br_3; (*7*) Yb_2Br_4; (*8*) Yb_2Br_5; (*9*) Yb_2Br_6; (a) stages I (1000 K) and (b) II (1100 K), respectively.

Composition and Pressure of Saturated Vapor

The partial vapor pressures were calculated by the standard procedure [13] using the relation:

$$p_j = \frac{kT}{\sigma_j^{\text{mol}}} \sum_i \frac{I_{ij}}{\gamma_i a_i}, \qquad (13)$$

where k is the sensitivity constant of the instrument, T is the cell temperature, σ_j^{mol} is the total ionization cross section of the jth molecule with the working energy of ionizing electrons (calculated on the basis of ionization cross sections σ_n^{at} of atoms n [25] using the expression $\sigma_j^{\text{mol}} = 0.75\sum_n \sigma_n^{\text{at}}$ [26]), $\sum_i (I_{ij}/\gamma_i a_i)$ is the total ion current of ions i of all types formed from molecule j (calculated on the basis of the resultant fragmentation coefficients (table)), a_i is the coefficient taking into account the natural abundance of isotopes of the measured ion, and γ_i is the coefficient of ion–electron conversion (it is assumed that $\gamma_i \sim M_i^{-1/2}$ [27], where M_i is the molecular mass of ion). The calculation results are presented in Figs. 4–8.

Vapor Composition upon the Vaporization of $YbBr_3$.

As can be seen in Fig. 4, such ytterbium-containing molecules as YbBr, $YbBr_2$, and $YbBr_3$ are present in the vapor in comparable amounts upon the vaporization of $YbBr_3$ at stage I. It is interesting to note that the partial vapor pressures of these molecules change almost identically with growing temperature, attesting with a high degree of probability to an identical mechanism of vaporization of di- and tribromide molecules; i.e., as a result of dissociation of $YbBr_3$ molecules on the surface of the sample under study, followed by desorption of the products into the vapor phase. On the other hand, a more substantial increase in partial pressures was observed for bromine atoms and molecules with increasing temperature (Fig. 4).

Estimating the relative content of atomic fractions of Yb and Br in vapor being $1.0 : 3.9_{\pm 0.2}$ for the highest temperature of the stage I allows us to conclude that the vaporization of $YbBr_3$ is incongruent.[3] It is the reduced bromine content in the sample being vaporized that is likely to predetermine the valence transformation of ytterbium Yb(III) → Yb(II) in the condensed phase,[4] i.e., the transition from stage I to stage II. Note that the temperature range (1100–1200 K) in which this transition takes place is close to the assumed melting temperature of $YbBr_3$ [12].

The higher molar fraction in the resulting $YbBr_2 : YbBr_3$ system corresponds to ytterbium dibromide by the beginning of stage II. Nevertheless, the molar fraction of $YbBr_3$ is not susceptible to any further reduction due to the occurrence of reaction (2). Additional support for this is the presence of Yb atoms in vapor at stage II (Fig. 4). The total vapor composition of ytterbium-containing particles upon the vaporization of $YbBr_3$ is presented in Fig. 5. The relative content of Yb and Br in vapor at stage II ($1 : 1.9_{\pm 0.2}$) demonstrates the brutto composition of the congruently vaporizing condensed phase, which can be presented as the triple system Yb–$YbBr_2$–$YbBr_3$, dibromide being its major component.

The presence of four components (Yb, YbBr, $YbBr_2$, and $YbBr_3$) in the vapor accounts for the wide variability of molecular associates Yb_2Br_2, Yb_2Br_3, Yb_2Br_4, Yb_2Br_5, and Yb_2Br_6 (in the spectrum, these correlate with the ions Yb_2Br^+, $Yb_2Br_2^+$, $Yb_2Br_3^+$, $Yb_2Br_4^+$, and $Yb_2Br_5^+$, respectively),[5] which are combinations of the specified simple components. This provides additional support for the occurrence of association/dissociation reactions in the surface layer.

In accordance with Dalton's law, when measuring the total saturated vapor pressure above ytterbium tribromide using the torsion-effusion method (without analyzing the vapor phase composition) we calculated the total pressure of molecules registered in the vapor upon the vaporization of $YbBr_3$ in order to compare our results with those obtained in [2] (Fig. 6). As can be seen in Fig. 6, the additive values of pressures

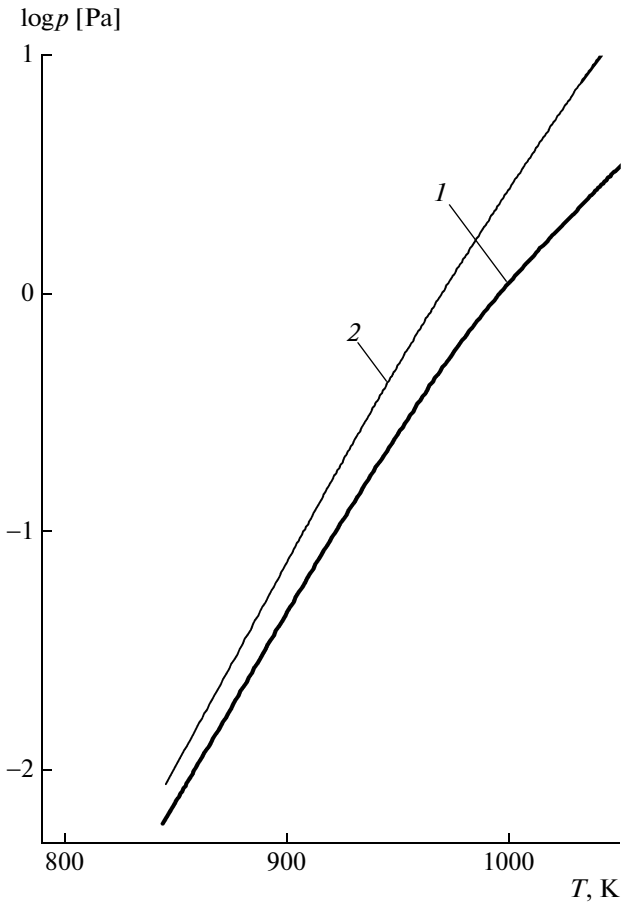

Fig. 6. Temperature dependence of total saturated vapor pressure upon the vaporization of $YbBr_3$: (*1*) our data; (*2*) data of [2].

obtained in this work are in close agreement with the data [2] obtained at low temperatures of the studied range. We believe the increasing pressure divergence at high temperatures can be attributed to the material of the effusion chamber. The authors of [2] used chambers made of pyrophyllite, which is likely to be a more inert material than graphite. As a result, the temperature range at which the transition from stage I to stage II takes place might shift. In preliminary experiments, we found that when a graphite cell is replaced with a molybdenum cell, this shift is approximately 100 K down the temperature scale.

Vapor Composition upon the Vaporization of $YbBr_2$

Upon the vaporization of ytterbium dibromide, such components as $YbBr_3$, $YbBr_2$, YbBr, Yb, Yb_2Br_2, Yb_2Br_4, and Yb_2Br_5 are present in the vapor; the highest vapor pressure was observed for monobromide molecules (Fig. 7). The total vapor composition in the vaporization of $YbBr_2$ is shown in Fig. 8.

[3] For low temperatures, this ratio is $1 : 2.9_{\pm 0.2}$, attesting within the experimental error to the congruent vaporization of $YbBr_3$ at these temperatures.

[4] The Knudsen method is a semidynamic technique in which even a small sampling of particular molecules can in certain cases play an important role during reactions in the condensed phase [28].

[5] In accordance with the well-known regularities for molecules of lanthanide halogenides Ln_2X_{2n} ($n = 1–3$) [17–21], the channel of dissociative ionization with the cleavage of one bromine atom and formation of $Yb_2Br_{2n-1}^+$ ions is most likely upon the interaction of such associates with electrons.

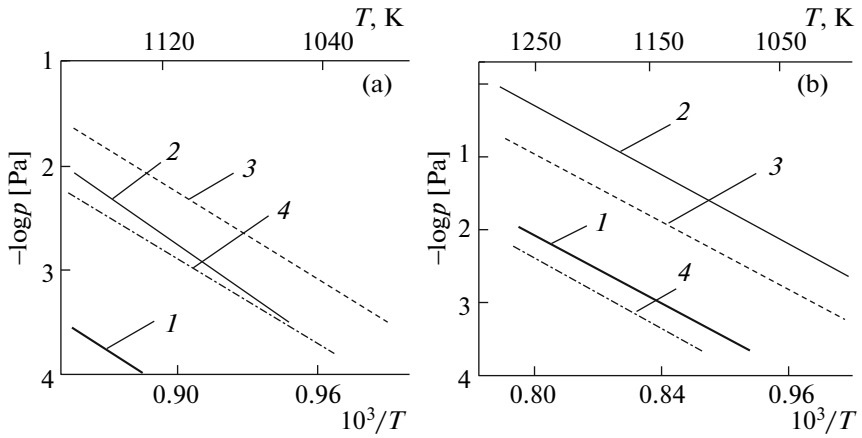

Fig. 7. Temperature dependences of partial pressures of vapor components upon the vaporization of $YbBr_2$: (*1*) $YbBr_3$; (*2*) $YbBr_2$; (*3*) YbBr; (*4*) Yb; stages (a) I and (b) II, respectively.

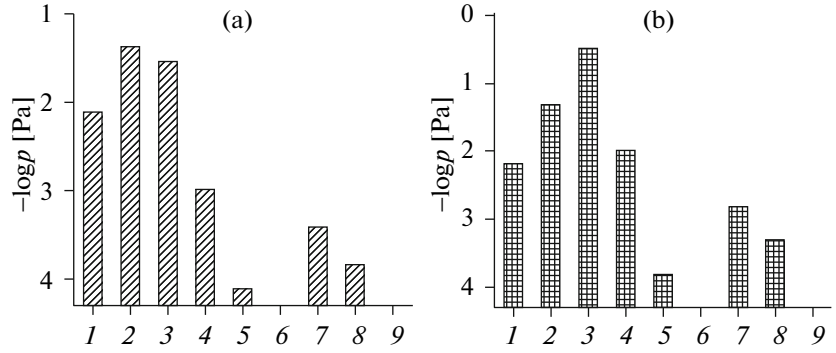

Fig. 8. Total vapor composition upon the vaporization of $YbBr_2$: (*1*) Yb; (*2*) YbBr; (*3*) $YbBr_2$; (*4*) $YbBr_3$; (*5*) Yb_2Br_2; (*6*) Yb_2Br_3; (*7*) Yb_2Br_4; (*8*) Yb_2Br_5; (*9*) Yb_2Br_6; stages (a) I (1175 K) and (b) II (1232 K), respectively.

The transition from stage I to stage II is accompanied by a considerable increase (by an order of magnitude) in the vapor pressures of $YbBr_2$ and $YbBr_3$ molecules and a proportional decrease in vapor pressure of Yb atoms, the vapor pressure of YbBr molecules remaining almost constant (Fig. 7). We may assume that the YbBr molecules are products of either the decomposition of $YbBr_2$ and $YbBr_3$ on the sample surface or their interaction with Yb atoms. The temperature range of the transition virtually coincides with the range between the stages upon vaporization of $YbBr_3$ (see above).

According to the vapor composition at stage I, the ratio between the atomic fractions of elements Yb : Br = $1.0 : 1.1_{\pm 0.2}$ attests clearly to the incongruent character of vaporization of $YbBr_2$ with the predominant loss of ytterbium in the condensed phase. At stage II, the elemental composition of the vapor changes considerably as compared with stage I; Yb : Br ratio is $1.0 : 1.9_{\pm 0.2}$. This composition does not undergo any further changes, evaporation becoming congruent. It is of great importance that this congruent composition (and the vapor composition) is identical to the congruent composition at stage II upon the vaporization of $YbBr_3$.

The complexity and diversity of chemical processes occurring in the condensed phase do not allow us to explicitly reveal the nature of the transitions observed upon vaporization of ytterbium di- and tribromides. Nevertheless, the results of this work agree with those of studies in which the vaporization of Yb–F systems was investigated [5, 6], proving conclusively that the initial ratio of lanthanide and halogen elements in the condensed phase in any case yields a certain congruently vaporizing composition. There is good reason to expect that the stoichiometry of this composition reflects the equality of the occurrence rates of reactions (1) and (2).

In order to support the reliability of our data on partial vapor pressures, the equilibrium constants K_p of gas phase reaction

$$2YbBr = YbBr_2 + Yb, \qquad (14)$$

calculated for stages I and II upon the vaporization of $YbBr_2$ are given in Fig. 9. It can be seen in Fig. 9 that there is close agreement between the K_p values within the experimental error at both stages.

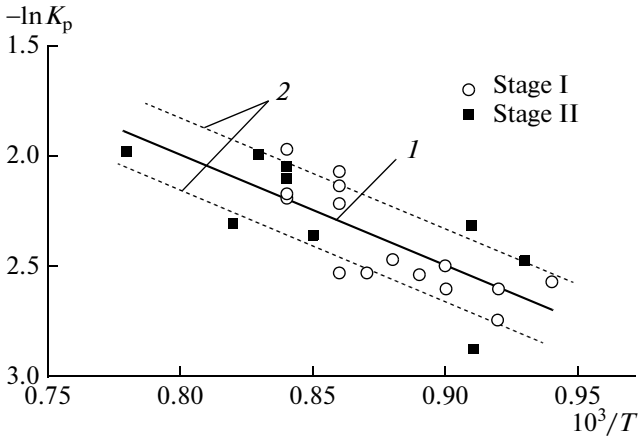

Fig. 9. Temperature dependence of equilibrium constant of reaction (14) for two stages of the evaporation of $YbBr_2$: (*1*) approximation line; (*2*) confidence interval ±10%.

ACKNOWLEDGMENTS

This study was supported by the Russian Foundation for Basic Research, project no. 09-03-97536.

REFERENCES

1. H. Oppermann and P. Schmidt, Z. Anorg. Allg. Chem. **631**, 1309 (2005).
2. B. Brunetti, A. R. Villani, V. Piacente, and P. Scardala, J. Chem. Eng. Data **50**, 1801 (2005).
3. C. Gietmann, G. Gigli, U. Niemann, and K. Hilpert, in *Electrochemical Society Proceedings 1997*, vol. 97–39, High Temperature Materials Chemistry (Electrochem. Soc., 1997), p. 657.
4. A. E. Grishin, A. S. Kryuchkov, M. F. Butman, et al., in *Proceedings of the 16th International Conference on Chemical Thermodynamics in Russia, RSST 2007, July 1–6, 2007, Suzdal'* ("Ivanovo," Ivanovo, 2007), Vol. 1, p. 190.
5. R. M. Biefeld and H. A. Eick, J. Chem. Phys. **63**, 1190 (1975).
6. T. Petzel and O. Greis, J. Less Common Metals **46**, 197 (1976).
7. G. Meyer, Chem. Rev. **88**, 93 (1988).
8. H. A. Eick, J. Less Common Metals **127**, 7 (1987).
9. G. Brauer, F. Weigel, H. Kühnl, et al., in *Handbook of Preparative Inorganic Chemistry*, in 6 vols., Ed. by G. Brauer (Academic Press, London, 1965; Mir, Moscow, 1985), Vol. 4, pp. 1166.
10. A. F. Holleman, *Lehrbuch Der Anorganischen Chemie*, Ed. by A. F. von Holleman and N. von Wiberg (de Gryuter, Berlin, New York, 1995), p. 1788.
11. I. V. Shakhno, Z. N. Shevtsova, P. I. Fedorov, and S. S. Korovin, *Chemistry and Technology of Rare and Scattered Elements*, Ed. by K. A. Bol'shakov (Vysshaya Shkola, Moscow, 1976), Ch. 2 [in Russian].
12. R. A. Lidin, V. A. Molochko, and L. L. Andreeva, *Constants of Inorganic Substances*, The Handbook, Ed. by R. A. Lidin (Drofa, Moscow, 2006) [in Russian].
13. L. N. Sidorov, M. V. Korobov, and L. V. Zhuravleva, *Mass-Spectral Thermodynamical Studies* (Mosk. Gos. Univ., Moscow, 1985) [in Russian].
14. A. M. Pogrebnoi, L. S. Kudin, A. Yu. Kuznetsov, and M. F. Butman, Rapid Comm. Mass Spec. **11**, 1536 (1997).
15. G. Meyer and M. S. Wickleder, *Handbook on the Physics and Chemistry of Rare Earth*, Ed. by K. A. Gschneidner and L. Eyring (Elsevier, Amsterdam, 2000), Vol. 28, Ch. 177, p. 53.
16. G. Meyer, Inorg. Synth. **25**, 146 (1989).
17. M. F. Butman, L. S. Kudin, V. B. Motalov, et al., Zh. Fiz. Khim. **82** (4), 631 (2008) [Russ. J. Phys. Chem. A **82**, 459 (2008)].
18. M. F. Butman, L. S. Kudin, V. B. Motalov, et al., Zh. Fiz. Khim. **82** (2), 227 (2008) [Russ. J. Phys. Chem. A **82**, 164 (2008)].
19. L. S. Kudin, M. F. Butman, V. B. Motalov, et al., Teplofiz. Vys. Temp. **46**, 388 (2008) [High Temp. **46**, 350 (2008)].
20. M. F. Butman, K. W. Krämer, L. S. Kudin, et al., Izv. Vyssh. Uchebn. Zaved., Khim. Khim. Tekhnol. **52** (7), 43 (2009).
21. Cl. Gietmann, K. Hilpert, and H. Nickel, *Thermodynamische Eigenschaften von Halogeniden der Lanthaniden* (Forschungszentrum Julich, Julich, 1997).
22. M. V. Kurepa, D. S. Babic, and D. S. Belic, Chem. Phys. **59**, 125 (1981).
23. J. W. Warren, Nature **165**, 810 (1950).
24. J. Nocedal and S. Wright, *Numerical Optimization*, 2nd ed. (Springer, Berlin, New York, 2006).
25. J. B. Mann, *Recent Developments in Mass Spectrometry*, Ed. by K. Ogata and T. Haykawa (Univ. Tokyo, Tokyo, 1970), p. 814.
26. *Thermodynamical Properties of Individual Substances*, The Handbook, in 4 vols, Ed. by V. P. Glushko (Nauka, Moscow, 1978–1984) [in Russian].
27. J. Drowart, C. Chatillon, J. Hastie, and D. Bonnell, Pure Appl. Chem. **77**, 683 (2005).
28. G. M. Rosenblatt, *Treatise on Solid State Chemistry*, Ed. by N. B. Hannay (Plenum, London, New York, 1976), Vol. 6A, Surface I, p. 165.